Measurement of high spatial resolution magnetocardiogram and source localization in rats with occlusion

S. Uchida, K. Goto, A. Tachikawa, K. Iramina, and S. Ueno

Department of Biomedical Engineering, Graduate School of Medicine, University of Tokyo,
7-3-1 Hongo, Bunkyo-ku, Tokyo, Japan

1 Introduction

In recent years, magnetocardiographic (MCG) source imaging has been implemented for the pathological studies of myocardial diseases. Many clinical studies on infarctions in humans were carried out [1]. A few studies, however, have reported on the *in vivo* experiments of basic myocardial diseases. Cohen [2] studied the ST sift and the DC shift of a dog's MCG, which were measured after an induced infarction by a balloon catheter. The source imaging was not estimated by MCG of the infarction.

In standard *in vivo* experiments, the subjects are small. Typical SQUID (superconducting quantum interference device) magnetometers consist of 15 mm to 20 mm diameter pick-up coils and the distance between each coil is 30 mm to 40 mm. When MCGs were measured by a typical magnetometer, the source images of the measured MCGs were distorted. A high spatial resolution magnetometer, however, is optimal for the measurement of MCGs since it is designed with small pickup coils and a short distance between the pickup coils and the subject.

Our 12 channel high resolution DC-SQUID (superconducting quantum interference device) gradiometer [3] has a higher resolution than the typical system because our system is constructed with 5mm diameter pick-up coils with a 7.5 mm distance between each coil. MCG and the auditory evoked magnetic fields in rats have been measured using our system.

In this study, MCGs in seven male rats were measured using our system in a magnetically shielded room before and after performing coronary artery occlusion. The source imaging was estimated by minimum norm estimation (MNE). Changes of the current source distribution before and after coronary artery occlusion were clarified.

2 Experimental design

The rats were measured using a 12-channel SQUID gradiometer in a magnetically shielded room (2.52 m length, 2.52 m width, 2.49 m height). The sensor layout and the pick-up coil in the gradiometer are shown in Figure 1. The diameter of the pickup coil was 5 mm. Twelve pick-up coils were located on a 7.5 mm grid. Each pick-up coil was a first order gradiometer with a 5 mm diameter and a 15 mm baseline. The distance between the pick-up coil and the bottom of the dewar was 5mm. A magnetically shielded room consisting of five 1 mm thick layers of permalloy and one 0.035 mm thick layer of copper was used. The field sensitivity was 100fT/√Hz in the white noise frequency range.

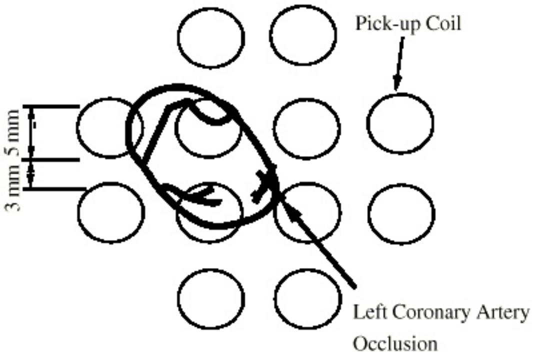

Figure 1: *12 areas of detected magnetic fields above a rat's heart and the design of pick-up coil.*

3 Coronary artery occlusion

Seven male rats (average±STD = 208 ± 10.95 g) were used in this study. The rats were anesthetized intraperitoneally with Urethane (1g/kg). A surgical ligation was performed during the experimentally induced myocardial infarction. After each rat had a tracheotomy, an artificial respirator was affixed to the rat at a respiration rate of 100 per minute and a ventilation volume of 2 ml per one respiration. After a left thoracotomy was performed, the left coronary artery was transfixed with silk sutures. The silk sutures were gently tied without stanching the blood flow in the coronary artery. Two strands of the silk anterior thorax sutures and anterior neck sutures were guided out through the pleural cavity.

4 Method and analysis

To improve the signal to noise ratio, magnetocardiogram signals were averaged over 1000 cardiac cycles. MCGs and the ECG were filtered from 0.5 Hz to 500 Hz and were sampled with 5000 Hz. Figure 1 shows 12 areas of detected magnetic fields above a rat's heart.

After MCGs of pre-occlusion were measured for 10 min, the occlusion was induced by tying two ends of the silk suture tightly. MCGs of post-occlusion were measured. The pre-analysis time course was for 5 min before the occlusion. The post analysis time course was from 5 min to 10 min after the occlusion. We calculated the primary current distribution of a rat's heart by minimum norm estimation (MNE) [4]. Magnetic fields $B = [b_1, b_2, ... b_M]^T$ is linearly related to the dipolar primary current distribution $Q = [q_1, q_2, ... q_N]^T$, where M is the number of sensors and N is the number of possible current source locations.

$$B=LQ \qquad (1)$$

where L is the lead field, B is determined from the magnetic fields, which were detected by 36 magnetometers. The conventional method can be written as follows:

$$Q = \Gamma^{-1}BL \qquad (2)$$

where

$$\Gamma = LL^T \qquad (3)$$

In practice, to decrease the numerical instability from noise, small eigenvalues of Γ were ignored. The cutoff value was defined as K (K<M).

The current space is assumed to be an elliptical surface.

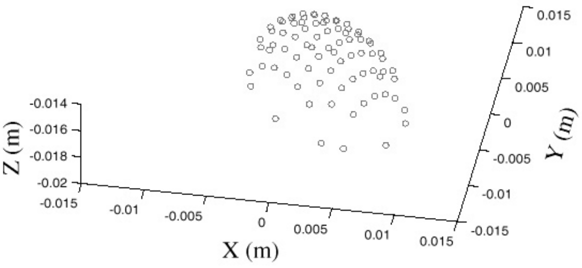

Figure 2: *Current space assumed to be an elliptical surface.*

5 Results

The waveforms of pre-and post-occlusion ECGs of a 200 g male rat are shown in Figure 3. The fine line indicates the ECG of pre-occlusion and the bold line indicates the ECG of post-occlusion. Increases in the electrical potential of the ST segment and T wave were measured after the left coronary occlusion. An increase in the electrical potential during the ST segment often appears in the diagnosis of myocardial infarction. Thus, the left coronary occlusion in this study was successfully achieved.

Figure 4 shows the waveforms of 12 pre- and post-occlusion MCGs. The fine lines indicate MCGs of pre-occlusion and the bold lines indicate post-occlusion MCGs. The magnetic fields of the 4th ch, 5th ch, 9th ch and 12th ch SQUID gradiometer increased during the ST segment and the T wave, whereas, the magnetic fields of the 10th ch and 11th ch decreased during the ST segment and the T wave.

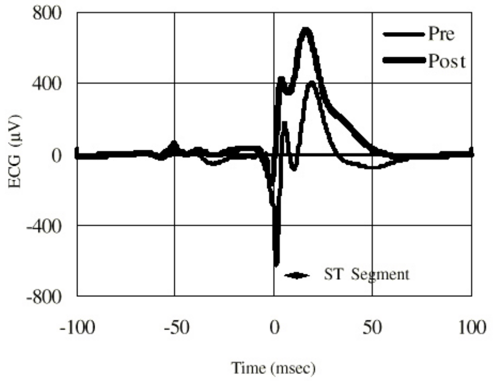

Figure 3: *Waveforms of ECGs of pre- and post-occlusion in a rat (male, 200g).*

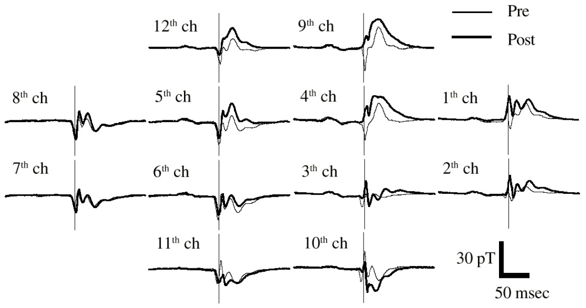

Figure 4: *Waveforms of 12 MCGs in pre- and post-occlusion (male, 200g). The fine line indicates MCG in pre-occlusion, the bold line indicates post-occlusion.*

For MCGs of pre- and post-occlusion in the ST segment and the T wave, the current distribution was calculated by MNE. Figures 5a and 5b show the pre- and post-occlusion current distribution in the ST segment, respectively. The arrows indicate the currents. The pre- occlusion currents had small amplitudes. Post-occlusion, however, the current distribution in ischemic area of the ventricular myocardium increased.

Figure 6 shows the significant increase of the current distribution between pre- and post-occlusion in the ST segment. The current distribution at the apex of the artery increased significantly.

In the normal case of the ST segment, the action potential of the ventricular myocardium is at a plateau. The current sources do not exist, because no potential gradient in the ventricular myocardium appears. In the ischemic case of the ST segment, the rapid repolarization occurs in the myocardial action potential [5]. We assumed that the potential gradient of the ventricular myocardium generated the magnetic fields.

a: Pre-Occlusion

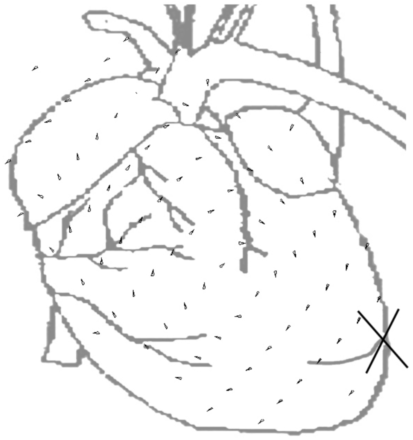

b: Post- Occlusion

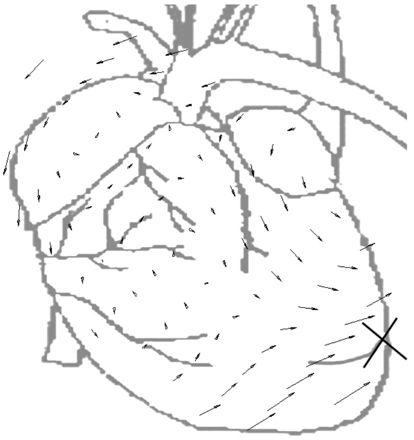

Figure 5*: The current distribution pre- (upper) and post- (lower) occlusion in ST segment. The arrows indicate the currents. The cross indicates the point of left coronary artery occlusion. Maximum current pre-occlusion was 5.2 nAm, post- was 12.9 nAm. The Cutoff value, K=6.*

Figures 7a and 7b show the pre- and post- occlusion current distributions in the T wave, respectively. Pre-occlusion currents of the left ventricular artery flowed in a downward left direction and post-occlusion currents shifted completely to the left. The direction of the currents is presented as a mirror image of the rat. The amplitude of the currents increased at post-occlusion.

Figure 8 shows the statistical results of the directions in the current distribution between pre- and post-occlusion in the T wave. The direction of the current distribution at the anterior ventricle changed to left after left ventricular coronary occlusion ($p<0.05$). The T wave is produced by the temporal difference of the repolarization between epi and endo myocardium [6], because the repolarization occurs more rapidly at the ischemic myocardium (left anterior) than for normal myocardium. We assumed that the large gradient potential of the left anterior region produced the currents that flowed to the left.

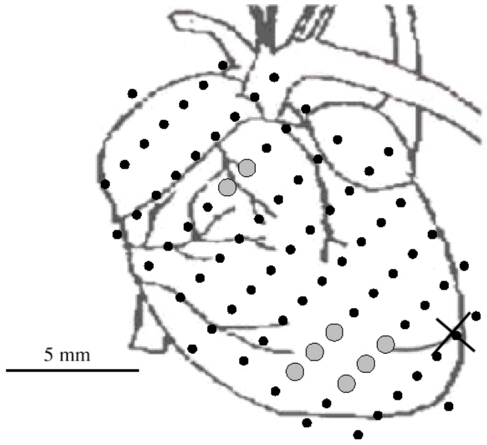

Figure 6: *The significant increase of the current distribution between pre- and post-occlusion in ST segment. The black points indicate positions in the current space. The circles indicate the position of the significant increase in the current distribution post- occlusion (p<0.05, paired t-test).*

6 Discussion

The MCGs of pre- and post- left coronary artery occlusion in rats were measured by a high resolution DC SQUID magnetometer. In the ST segment, the current distribution significantly increased at the ischemic area. In the T wave, the direction of the current distribution clearly shifted to the left. Our results support the simulations of the infarction model by Killmann [7] and Czapski [8].

In the *in vivo* study, Cohen [4] measured the base line shift and the ST segment shift of magnetocardiograms in coronary occlusion, and a shift to a zero current during the ST segment. Changes of the MCGs waveforms in the ST segment resembled our results. The occlusion generally produces a primary steady current in the affected area of the myocardium during the ST segment, which causes an interruption of the current during ventricular depolarization. Unlike our study, Cohen did not calculate the current source of the ischemic area.

In conclusion, the large gradient potential of the left anterior region by the ischemic action potential produced the current changes. Our system will promote and develop future *in vivo* studies on myocardial ischemia.

a: Pre-Occlusion

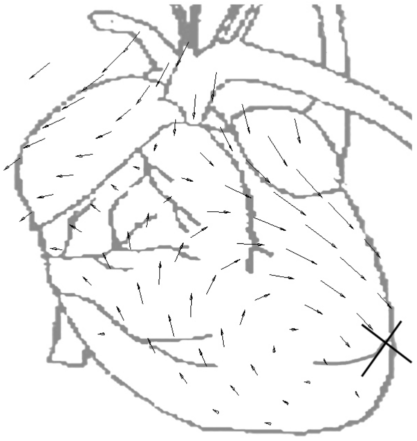

b: Post-Occlusion

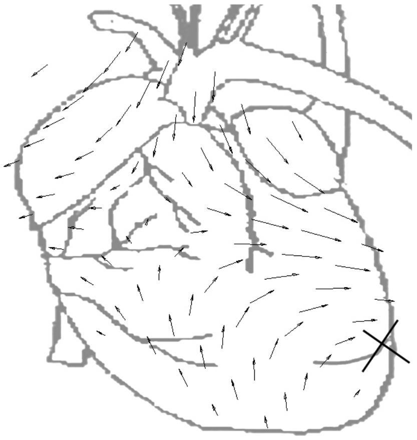

Figure 7*: The current distribution pre- (upper) and post- (lower) occlusion in T wave. The arrows indicate the currents. The cross indicates the point of left coronary artery occlusion. Maximum current pre-occlusion was 12.5 nAm, post- was 13.2 nAm. The Cutoff value K=6.*

References

1. M. Mäkijärvi*, et al,* "Detection and localization of myocardial ischemia and viability by magnetocardiography"*,* in *Recent Advances in Biomagnetism,* T. Yoshimoto et al Eds. Sendai: Tohoku University Press, 1999, pp. 929-932.

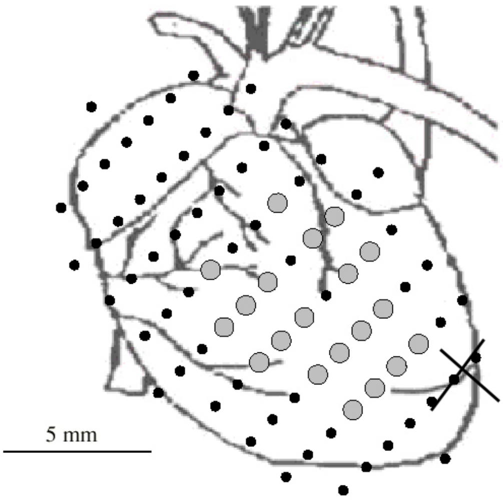

Figure 8: *Clear changes of the direction of the current distributions between pre- and post-occlusion in ST segment. The black points indicate positions in the current space. The circles indicate the position of the currents flowing to the left in the post-occlusion current distribution significantly (p<0.05, paired t-test).*

2. D. Cohen and L.A. Kaufman, "Magnetic Determination of the relationship between the S-T segment shift and the injury current produced by coronary artery occlusion", *Circ. Res.* **36,** 414-424, 1975.
3. K. Iramina, et al, "Measurement of Biomagnetic Fields Using a High Resolution DC-SQUID Magnetometer", *J. Appl. Phys.* **83**, 6465-6467, 1998.
4. M.S. Hämäläinen and R.J. Ilmoniemi: "Interpreting magnetic field of the brain: minimum norm estimates", *Med. Biol. Eng. Comput.* **32**, 35-42, 1994.
5. R.P. Holland and J.P.R. Brooks: "Precardial and epicardial surface potentials during myocardial ischaemia in the pig", *Circ. Res.* **37**, 471-480, 1975.
6. M.R. Franz, et al: "Monophasic action potential mapping in human subjects with normal electrocardiograms: Direct evidence for the genesis of T wave", *Circ.* **75**, 379-386, 1987.
7. R. Killmann, et al, "Localisation of myocardial ischaemia from the magnetocardiogram using current density reconstruction method: computer simulation study", Med. Biol. Eng. Comput. **33**, 643-651, 1995.
8. P. Czapski, et al, "MCG simulation of myocardial infarctions with realistic heart-torso model", *IEEE Trans. Biomed. Eng.* **45** 11, 1313-1321, 1998.